Effect of Cross-Links on the Phase Separation Behavior of a Miscible Polymer Blend

Robert M. Briber* and Barry J. Bauer

Polymers Division, Institute for Materials Science and Engineering, National Bureau of Standards, Gaithersburg, Maryland 20899. *Received January 22, 1988; Revised Manuscript Received April 26, 1988*

ABSTRACT: The effect of radiation cross-linking on the phase diagram and scattering function for a compatible polymer blend of deuteriated polystyrene and poly(vinyl methyl ether) has been examined by small angle neutron scattering. The scattering curves for the cross-linked blends exhibit a maximum at a nonzero q vector, the position of which depends linearly on the square root of the radiation dose or inversely on the square root of the number of repeat units between cross-links, $N_c^{1/2}$. This dependence was predicted by de Gennes, but the measured position of the maximum is smaller than predicted. The spinodal temperature can be determined by plotting the inverse of the scattered intensity at the maximum, $S(q^*)^{-1}$, versus inverse temperature and extrapolating to the point where $S(q^*)^{-1} = 0$. The inverse of the measured spinodal temperature depends linearly with radiation dose or with N^{-1} as predicted. This increases the size of the single phase region of the phase diagram with the extrapolated spinodal temperature increasing from 149 °C for the uncross-linked blend to 430 °C for the blend with a radiation dose of 125 Mrad. The theory by de Gennes predicts that the scattered intensity at $q = 0$ equals 0 for the cross-linked blends which is not observed experimentally.

Introduction

The phase separation behavior of miscible polymer blends and block copolymers has been the topic of many recent papers in the literature. Small angle neutron scattering (SANS) has emerged as one of the most important experimental tools for examining the concentration fluctuations present in polymer blends in the one phase region as the spinodal is approached.[1-7] Studies of these types provide information on the critical exponents, the magnitude of the interaction parameter, χ, the spinodal temperature, and the single chain scattering function for the components of the blend. The success of these experimental studies is partially due to the ability to interpret the scattering data using mean field theories developed by de Gennes[8] and Benoit et al.[9] for linear blends and by Leibler,[10] Kawasaki,[11] and Olvera de la Cruz and Sanchez[12] for block copolymers of various architectures. Work on block copolymers has demonstrated that the effect of coupling two dissimilar chains together at a single junction is to increase the single phase region of the phase diagram relative to that of the blend of the corresponding linear materials.

In this paper we study the effect of cross-linking (by γ-ray irradiation) on the concentration fluctuations in a compatible polymer blend. The effect of cross-linking on the scattering function and spinodal temperature is examined as a function of the cross-link density for a set of samples of constant composition close to the critical composition for the compatible polymer blend of deuteriated polystyrene (PSD) and poly(vinyl methyl ether) (PVME). We find that cross-linking greatly increases the single phase region of the phase diagrams and that the main features of the observations are consistent with predictions by de Gennes.[13]

Background

The PSD/PVME system exhibits a lower critical solution temperature (phase separation upon heating) and has a critical composition shifted toward the PVME-rich side of the phase diagram.[1,14] This system has been the focus of numerous papers in the recent literature including a number of SANS studies.[1-3,14] It should be noted that the PSD/PVME system is not equivalent to the hydrogenated PS/PVME system with the phase boundary for the latter system occurring at lower temperatures by about 40 °C.[15] The effect of cross-links on compatible polymer blends has been addressed by only a few authors.[16,17] Most of this work has centered on the area of interpenetrating polymer networks (IPN), but it should be noted that IPNs are fundamentally different from the system discussed in this paper.[16-18] The concept of an IPN implies two independently cross-linked networks with no cross-links between the components (no A–B cross-links) or, as with the case of an semi-IPN, only one cross-linked network mixed with a second component that remains linear (only A–A cross-links). In the system discussed in this paper the compatible polymer blend of linear materials is cross-linked by γ-rays which introduces all the different types of cross-links (A–A, B–B, and A–B). In addition, the IPNs studied in the literature are almost exclusively phase separated with truly compatible IPNs being rare.[17,19,20] The effect of exclusively A–A cross-links on the phase diagram and concentration fluctuations in a compatible polymer blend is an interesting question in itself and will be addressed in a different publication.[19,20]

Theory

Radiation Cross-Linking. γ-ray irradiation has long been used to cross-link polymers.[21] The process involves the polymer absorbing a high-energy photon and ejecting an electron. This leaves a radical ion that is capable of a variety of high-energy reactions, the exact nature of which can be quite complicated. It was our goal to use irradiation as a tool for producing cross-linked samples; consequently we were not concerned with the exact mechanism of the reaction. For the analysis all possible reactions were grouped into two classes, the first causing a chain to break (two reactions involved, one for each chain type in the blend) and the second causing a cross-link to be formed (three cases, A–A, B–B, and A–B types).

When a polymer with relatively narrow molecular weight distribution undergoes an appreciable amount of both cross-linking (branching when one is below the gel point) and chain scission on exposure to high-energy radiation, the molecular weight distribution noticeably broadens at both the high and low molecular weight regions.[22] Chains that are broken into smaller units have a lower probability of becoming attached to another chain due to their smaller size and show up in the results from gel permeation

* To whom correspondence should be addressed.

chromatography (GPC). The absence of an increase in low molecular weight material in a GPC analysis means that chain scission is negligible in comparison to branching (cross-linking).

The fraction of the repeat units in a high molecular weight polymer crosslinked by radiation at moderate doses that undergo branching is very small (all the samples studied in this paper fall in this category). It is therefore reasonable to assume that the repeat units are not consumed by the irradiation and that the probability of a unit being branched is proportional to the dose it has received

$$P = KD \tag{1}$$

where P is the probability, D is dose, and K is the proportionality constant. The probability that a chain is not branched can be calculated by assuming the probabilities of all N repeat untis (N is the number of units per chain) to be equal

$$P(\text{not branched}) = (1 - P)^N = (1 - KD)^N \tag{2}$$

If the polymer has a molecular weight distribution $W(N)$, the fraction of polymer not branched after dose D is

$$W_D/W_0 = \int_0^\infty (1 - KD)^N W(N)\, dN \tag{3}$$

where W_D is the weight unbranched after dose D and W_0 is the total initial weight. A commonly used molecular weight distribution is the Zimm–Schultz distribution.[23,24] It is a two-parameter distribution, N_w being the weight average degree of polymerization and N_n being the number average. The distribution is given by eq 4 where k =

$$W(N) = (y^k/\Gamma(k))N^{k-1} \exp(-yN) \tag{4}$$

$N_w/(N_w - N_n)$, $y = k/N_w$, and Γ is the gamma function. The fraction unreacted after dose D is therefore

$$W_D/W_0 = (y/(y - \ln(1 - KD)))^k \approx (y/(y + KD))^k \tag{5}$$

and a plot of $(W_D/W_0)^{-1/k} - 1$ versus D passes through the origin and has a slope of K/y. The change in the amount of unbranched polymer can be followed by GPC and will be described later.

Although PSD and PVME form a compatible blend, they have quite different solubility properties. Toluene acts as a good solvent for both polymers, but methanol is a good solvent for PVME and a nonsolvent for PSD. An uncross-linked blend of PSD and PVME can be dissolved in toluene and precipitated into methanol. The blend should be separated quantitatively into the starting components, with the PSD precipitating and the PVME staying in soluition. However, an irradiated blend at low doses will contain A–B type branching resulting in graft copolymers that cannot be separated by this method. Instead of being pure components after precipitation into methanol, each phase will contain some of the graft copolymer.

After the precipitation, all of the nongrafted polymer of the two types will go into the soluble or insoluble phase depending on the polymer type. The graft polymer will partition itself between the phases. The partitioning will be molecular weight dependent, with lower molecular weight grafts being more likely to be brought along into an unfavorable phase than one with high molecular weight. The problem is complicated by the fact that four components are present and therefore six interaction parameters need to be known. Since the interaction parameters are not known, the approximation is made that the molecular weight distributions of each grafted polymer is the same in each phase. This makes it a limiting case, and the A–B cross-link probabilities calculated by this method are a minimum value.

If w_1 is the weight of PSD in the PMVE rich phase and w_2 is the weight of PVME in the PSD rich phase, the starting blend has 30 wt % PSD and 70 wt % PVME, and α is the fraction of the graft copolymer partitioned into the PVME rich phase, then eq 6 and 7 hold if the partitioning of molecular weights are equal. The values of the rate constants are related with $0.3k_{PSD}/58 = 0.7k_{PVME}/112$. The partitioning fraction α can be eliminated between eq 6 and 7. For any given composition of the two phases and given dose, the rate constants can be calculated.

$$w_1 = 0.3\alpha(y_{PSD}/(y_{PSD} + K_{PSD}))^{k_{PSD}} \tag{6}$$

$$w_2 = 0.7(1 - \alpha)(y_{PVME}/(y_{PVME} + K_{PVME}))^{k_{PVME}} \tag{7}$$

Scattering. P.-G. de Gennes has published in a short note the only theoretical investigation on the effect of A–B cross-links on the concentration fluctuations and phase diagram for a compatible polymer blend.[13] The theory is based on the classical Flory–Huggins formulation for the free energy of a compatible polymer blend.[25,26] de Gennes assumes that the blend is cross-linked randomly with exclusively A–B cross-links to produce a network but states that the presence or absence of A–A or B–B cross-links should not change the results, at least qualitatively. The number of monomer units between cross-links is given by N_c where $N_c \ll N$ and N is the degree of polymerization of the starting blend (assuming $N_A = N_B$). The requirement of $N_c \ll N$ is to assure that the system is not close to the gel point. For simplicity de Gennes also assumes that the composition (volume fraction) of the blend is $\phi_A = \phi_B = 0.5$. The retractive force of the network generated when the blend attempts to phase separate is calculated in analogy with the separation of charges in a dielectric medium. He then writes the free energy in terms of its Fourier components which allows the evaluation of the scattering function, $S(q)$, for the system in the one phase region. This scattering function is given by

$$S(q)^{-1} = \frac{C}{q^2} + \tfrac{1}{2}(\chi_0 - \chi) + \frac{b^2q^2}{24} \tag{8}$$

where χ_0 is the critical value of χ for the uncross-linked blend, b is the step length for the polymer chains (the values of b for the two components are assumed to be equal), q is the scattering vector ($q = (4\pi \sin\theta)/\lambda$), and C is related to the "internal rigidity" of the chains to which de Gennes gives an approximate value of $C \approx 36/(N_c^2b^2)$. $S(q)$ in eq 8 is qualitatively very similar to the one derived by Leibler for diblock copolymers in the single phase region.[10] Leibler has shown that the scattering function for diblock copolymers in the small and large q limits consists of q^2 and q^{-2} terms which have the form $2N^2b^2f^2(1 - f)^2q^2/3$ as $q \to 0$ and $12f(1 - f)/q^2b^2$ as $q \to \infty$ where N is the total degree of polymerization of the block copolymer and f is the fraction of the A species in the block copolymer. These limits are in direct analogy to the q^2 and q^{-2} terms in eq 8 except that de Gennes developed eq 8 for the symmetric case where $\phi_A = \phi_B$ so the dependence of $S(q)$ on blend concentration is not present.

$S(q)$ as described by eq 8 will exhibit a maximum at a nonzero q vector (termed q^*). This is in contrast to the scattering function for a blend of linear polymers which has a maximum at $q = 0$. This maximum in the scattering function at q^* has been termed the correlation hole effect by de Gennes.[8] The maximum in $S(q)$ can be understood by noting that eq 8 indicates $S(q = 0) = 0$ which is due to the chains being cross-linked to each other and cannot

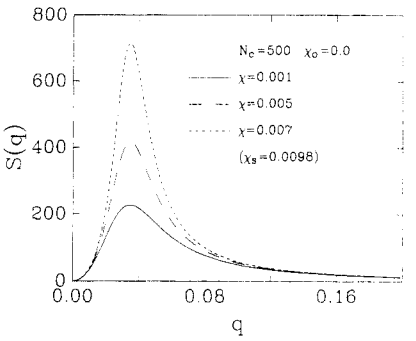

Figure 1. Plot of the scattering function $S(q)$ versus q given by eq 8 for three different values of χ.

phase separate at infinite wavelengths (i.e. cannot macrophase separate) but instead are constrained to undergo microphase separation at a length scale approximated by q^*. As the value of χ approaches the critical value, χ_s, the peak in the scattering function increases in intensity until it diverges at $\chi = \chi_s$, which corresponds to the spinodal temperature. This prediction is interesting to compare to the case of block copolymers where if there is a relatively large distribution of block lengths present the peak in the scattering function will disappear due to macrophase separation of the block copolymers with different compositions.[5,27] In a cross-linked blend the system cannot macrophase separate; hence the scattering function cannot diverge at infinite wave vector ($q = 0$) and microphase separation should be expected even though the system has a broad distribution of length scales.

Figure 1 is a plot of the scattering function given by eq 8 for a cross-linked blend with $N_c = 500$, $b = 8$ Å, and $\chi_0 = 0$ (corresponding to infinite molecular weight of the starting blend). The three curves correspond to $\chi = 0.001$, 0.005, and 0.007 for the least intense to the most intense, respectively. The value of χ at the spinoidal is $\chi_s = 0.0098$.

The position of the maximum in $S(q)$ can be found by taking $\partial(S(q)^{-1})/\partial q = 0$ and solving for $q = q^*$

$$(q^*)^4 = \frac{864}{N_c^2 b^4} \tag{9}$$

or equivalently $q^* = 5.42/(N_c^{1/2}b)$. The value of $\chi = \chi_s$ at the critical point can be calculated from eq 8 by setting $S(q^*)^{-1} = 0$ (the scattering function diverges at q^* at the critical point).

$$\chi_s - \chi_0 = 2\sqrt{6}/N_c \tag{10}$$

If we note that for a symmetric linear blend $\chi_0 = 2N^{-1}$ and we examine the special case where $N = N_c$, then eq 10 becomes

$$\chi_s N_c = 2 + 2\sqrt{6} \tag{11}$$

This violates the assumption originally made by de Gennes that $N_c \ll N$ which was done in order to assure that the system was not close to the gel point (to limit the effect of unattached chains and chain ends). We could keep the requirement of being beyond the gel point and still allow $N = N_c$ if the system was cross-linked by the end linking of the chains in a polymer blend. Equation 11 indicates that the critical value of χ for phase separation is increased significantly over that for a blend of linear polymers. For the case where the blend is cross-linked by radiation so that $N_c \ll N$, then the single phase region of the phase diagram is greatly increased because of the effect of N_c which is decreasing in proportion to the radiation dose.

If we evaluate the scattering function at q^* by substituting eq 9 into eq 8 and use the relation for χ_s given in eq 10, one obtains the scattered intensity at q^* diverging as the spinodal is approached with the form

$$S(q^*)^{-1} \sim (\chi_s - \chi)^{-\gamma} \tag{12}$$

where $\gamma = 1$ as expected for a mean field system.[28]

If we assume that the Flory interaction parameter is inversely proportional to temperature $\chi \sim T^{-1}$, then a plot of the scattered intensity at q^* versus T^{-1} should be linear. This is in direct analogy with the mean field behavior observed for linear polymer blends where the scattering function diverges at $S(q = 0)$ rather than at a nonzero q vector. The assumption that χ varies as T^{-1} also leads to the prediction from eq 10

$$\frac{1}{T_s} = \frac{2\sqrt{6}}{N_c} + \frac{1}{T_0} \tag{13}$$

where T_s is the critical (or spinodal) temperature for the cross-linked blend with N_c units between cross-links and T_0 is the critical temperature for the uncross-linked blend. The analysis by de Gennes only defines the limit of the unstable region of the phase diagram (i.e. the spinodal). No attempt is made to calculate the limits of metastability (as defined by the coexistence curve) or the equilibrium morphologies that might develop as a consequence of phase separation.

Experimental Section

It was desirable to use the highest molecular weight polymers available for the SANS experiments in order to minimize the effects of unattached chains and to attain gelation of the blend at relatively low radiation dose. This would also help to meet the criterion of $N_c \ll N$ as discussed in the Theory section.

The PVME was polymerized cationically with boron trifluoride–ethyl ether complex as a catalyst and fractionated with toluene as the solvent and heptane as the nonsolvent.[29] The highest molecular weight fraction obtained was used for the SANS experiments and had $M_w = 1\,690\,000$ g/mol. The PSD used in the SANS experiments was prepared by emulsion polymerization. A 25-mL flask was charged with 2.0 mL of styrene-d_8, 3.0 mL of a 2 wt % $K_2S_2O_8$ solution in boiled water, and 0.3 mL of a 0.5 wt % solution of sodium lauryl sulfate in boiled water. The reaction flask was purged with argon and held at 32 °C for 4 days. The reaction mixture was then added to a saturated NaCl solution in water to break the emulsion. The polymer was purified by dissolving in toluene and subsequent precipitation into methanol. This was repeated twice. GPC of the PSD indicated a very high molecular weight, several times higher than the PVME (M_w(PSD) > 4 000 000). The PVME used for the study of the radiation cross-linking kinetics had $M_w = 120\,000$ and $M_w/M_n = 1.2$. The PSD used for the kinetics study was purchased from Polymer Laboratories and had $M_w = 460\,000$ and $M_w/M_n = 1.25$.[30]

The SANS samples were made by dissolving 30 wt % PSD and 70 wt % PVME in toluene. This composition was chosen to be close to the critical point in order to have the spinodal temperature for the uncross-linked material to be at as low a temperature as possible and to have the experiments match with the scattering theory (which was developed for a system at the critical point). The PSD/PVME system is asymmetric with respect to the position of the critical point due to the composition dependence of χ.[1-3,14] A thin (ca. 0.1-mm) film was cast and then dried under vacuum. Disks were cut out from the film and then stacked and pressed at 120 °C into the spacer rings that would be used for the scattering experiment. The samples were pumped down on a high vacuum line in glass ampules. The ampules were heat sealed on the line and were irradiated at the NBS Co^{60} γ-ray source. Four samples were prepared for SANS-labeled 0MR, 25MR, 50MR, and 125MR each receiving a dose of 0, 25, 50, and 125 Mrad, respectively. The dose rate was about 1 Mrad/h. The irradiation temperature was not precisely controlled but was approximately 45 °C.

The blends for the cross-linking kinetics study (30/70 PSD/PVME wt %) were cast in the form of thin films (ca. 0.5 mm)

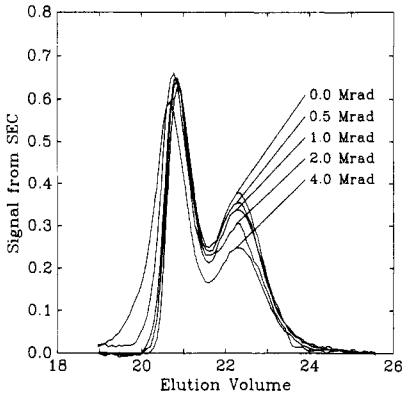

Figure 2. GPC traces for the blends irradiated for doses less than the gel point.

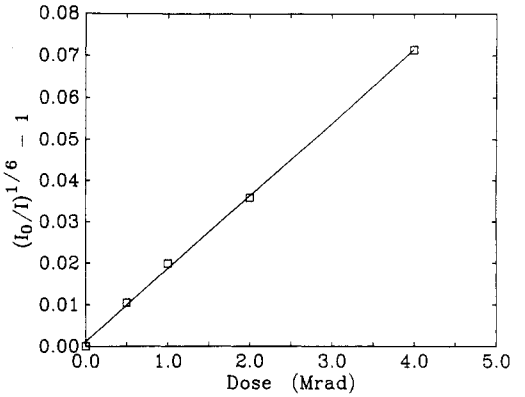

Figure 3. Plot of the disappearance of the GPC peak for PVME in Figure 2 versus dose.

which were sealed in glass ampules under vacuum and irradiated. Doses were 0, 0.5, 1.0, 2.0, and 4.0 Mrad.

All of the samples used in the study of the radiation cross-linking kinetics were soluble in toluene. They were dissolved (in toluene) and precipitated into methanol and allowed to settle, and the solids were filtered off. Their composition was characterized by FTIR using integrated absorbance peaks to estimate the mass present. The PSD absorption was integrated between 2140 and 2225 wavenumbers and the PVME from 2785 to 2849 wavenumbers, these peaks being relatively strong and independent. Blend samples of various known compositions were also made from the same polymers as used for the kinetics study to determine eq 14 and 15 for relating absorbance to concentration. Equation 14 was fit for samples with low PSD concentration and eq 15 for samples with low PVME content.

$$ABS_{PSD}/ABS_{PVME} = 0.0033 + 0.2783(w_{PSD}/w_{PVME}) \quad (14)$$

$$ABS_{PVME}/ABS_{PSD} = -0.078 + 0.350(w_{PVME}/w_{PSD}) \quad (15)$$

$ABS_{PSD\ or\ PVME}$ is the integrated absorbance over the range mentioned previously, and $w_{PSD\ or\ PVME}$ is the weight fraction of the specified component.

The scattering experiments were carried out at the NBS small angle neutron scattering facilities using conditions identical with previous work done with linear PSD/PVME blends.[1,2] The wavelength of the incident neutron beam was 6 Å with $\Delta\lambda/\lambda$ = 25% as determined by using a velocity selector. The data were collected by using a two-dimensional x-y detector, and the data were stored and reduced on various laboratory computers.

Results and Discussion

Figure 2 shows a GPC chromatogram for the five blend samples used for the kinetics study, all normalized to the same total area. The material to elute first is the higher molecular weight PSD component followed by the PVME. As seen in Figure 2 the peak due to the PVME decreases with increasing dose. The branched PVME has a larger hydrodynamic volume that the starting PVME and shifts the curve to the left. If the shift is great enough, the height of the peak is proportional to the amount of unbranched PVME. If the peak height for the PVME in Figure 2 is taken to be proportional to the amount of PVME present, then equating peak height to I in eq 5 (I_0 is the peak height at zero dose) allows $(I_0/I)^{-1/k}$ versus dose to be plotted as in Figure 3 where $k = 6$ for the PVME used in this study. The slope of the line gives $P = 5.10 \times 10^{-5}$ D with P being the probability of a PVME repeat unit being branched to either another PVME or PSD unit.

In Figure 2, there is no evidence of an increase of low molecular weight PVME; therefore chain scission of the PVME is occurring in only minor amounts and can be considered negligible. Pure PVME has been shown to undergo cross-linking rather than chain scission when exposed to γ-rays.[31] GPC chromatograms of the methanol insoluble fraction for the samples with 0, 0.5, and 1.0 Mrad dose also shows no increase in low molecular weight material, indicating that chain scission of PSD is also a minor reaction as has been shown for protonated polystyrene.[21] The PSD peak position shifts slightly to the left, indicating an increase in the PSD molecular weight.

Table I
Compositions of Fractionated Irradiated PSD/PVME Blends[a]

	W_{PSD}	
dose (Mrad)	methanol insoluble	methanol soluble
0.0	1.007	−0.007
0.5	0.949	0.051
1.0	0.898	0.041

[a] PVME M_w = 120 000 g/mol, PSD M_w = 530 000 g/mol, and PSD/PVME = 0.3/0.7.

Table I shows the results from the fractionation experiments. Equation 14 was used to estimate the PSD content in the PVME rich phase, and eq 15 was used to calculate the PVME content in the PSD rich phase. For the sample with no irradiation, FTIR also indicates within the uncertainties involved that complete separation of the PSD and PVME was achieved. At 0.5 and 1.0 Mrad, considerable grafting is present since each phase now contains both polymers. For the 2.0 and 4.0 Mrad samples the fractionation procedure yielded an emulsion upon precipitation into methanol. The 2.0 and 4.0 Mrad samples could not be separated into methanol soluble and insoluble components.

The minor components in each of the separated phases for the 0.5 and 1.0 Mrad samples were due to creation of PSD–PVME graft copolymers, where the moles of PSD brought into the methanol soluble phase (PVME rich phase) and moles of PVME brought into the methanol insoluble phase (PSD rich phase) was the result of an equivalent number of PSD–PVME cross-links. For polymers with molecular weight distributions, eq 6 and 7 can be used to estimate the probability that a PVME unit is linked to a PSD unit, assuming that the molecular weight distributions partition equally into the two phases. Since low molecular weight grafts are more likely to be brought into a phase of the opposite polymer type than high molecular weight ones, the calculations represent a limiting case, with the actual number of cross-links being greater than the value calculated based on the assumption of equal partitioning.

This leads to an estimate from FTIR of the probability of a PVME being joined to a PSD to 3.2×10^{-6} D. Table II lists the SANS samples studied in this work, along with the values of molecular weight and degree of polymerization between cross-links. Two values of N_c were calculated: one based on the GPC experiments (higher bound) and

Table II
Characterization of PSD/PVME Irradiated Blends[a]

sample	dose (Mrad)	M_c(PVME)[b]	N_c(PVME)	M_c(PSD)	N_c(PSD)	method	N_c(av)[c]
0MR	0						
25MR	25	45 000	780	19 000	170	GPC	
		71 000	1200	31 000	270	FTIR	870
50MR	50	23 000	390	9 800	90	GPC	
		36 000	610	15 000	140	FTIR	440
125MR	125	9 000	160	3 900	40	GPC	
		14 000	250	6 100	60	FTIR	180

[a] PVME M_w = 1 690 000 g/mol, PSD M_w > 4 000 000 g/mol, and PDS/PVME = 0.3/0.7. [b] Molecular weights and degrees of polymerization given are number averages. [c] $N_c(av) = [[N_c(PVME)^2 + N_c(PSD)^2]/2]^{1/2}$ where N_c(PVME or PSD) = N_c(FTIR).

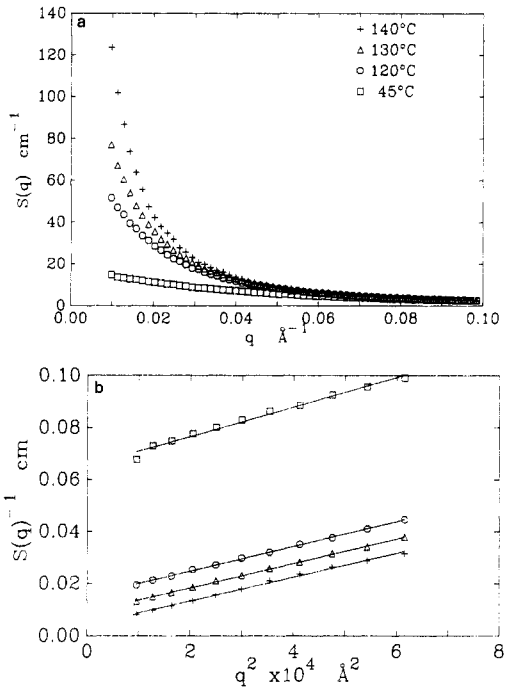

Figure 4. (a) $S(q)$ versus q at different temperatures for sample 0MR. (b) $S(q)^{-1}$ versus q^2 from the data in 4a.

one based on the FTIR experiments (lower bound). It should be emphasized that these values are only rough estimates due to the assumptions necessary in the measurements. The molecular weights listed are number average values.

Figure 4a is a plot of $S(q)$ versus q for sample 0MR, the unirradiated blend, as a function of temperature. As the temperature is raised, the scattering increases as the spinodal is approached. At small q the scattering from a single phase linear blend has been shown to follow classical Ornstein–Zernike behavior given by eq 16[1-3]

$$S(q) = \frac{S(0)}{1 + \xi^2 q^2} \tag{16}$$

where $S(0)$ is the scattered intensity at zero angle ($S(q = 0) = S(0)$ and ξ is the correlation length. As the spinodal is approached, both $S(0)$ and ξ diverge as expected for a mean field system.[28] A plot of $S(q)^{-1}$ versus q^2 should be linear and allow determination of $S(0)$ and ξ. Figure 4b shows such a plot for sample 0MR over the range (0.0098 Å^{-1} ≤ q ≤ 0.025 Å^{-1}). As expected the data are linear, indicating that the scattering obeys eq 16. Equation 16 is only strictly valid for $qR_g \ll 1$, and to analyze the data in detail the full structure factor as given by de Gennes for a linear polymer blend should be used for sample 0MR.[8] This full analysis has been done for sample 0MR, and the value of T_s is within 3 °C of that determined from the analysis using eq 16. Since the object of this paper is not a detailed discussion of the scattering from linear blends of PSD and PVME (see ref 1–3), this analysis will not be presented, and for simplicity we will use eq 16. Values of $S(0)$ and ξ determined from Figure 4b are given in Table III. $S(0)$ should behave in the same manner as $S(q^*)$ given in eq 11 so a plot of $S(0)^{-1}$ versus T^{-1} should allow extrapolation to the spinodal temperature where $S(0)^{-1} = 0$.

Table III

	0MR		S(q^*) (cm)		
T (°C)	$S(0)$ (cm)	ξ (Å)	25MR	50MR	125MR
45	15.4	30			
120	65.8	56	19.4	16.0	11.8
130	112.3	73	19.8	18.2	12.7
140	239.8	108	22.0	21.2	13.5
150			24.8	23.7	14.5
160			27.4	26.1	14.8
170			33.6	29.0	15.9
180			46.9	31.8	17.2

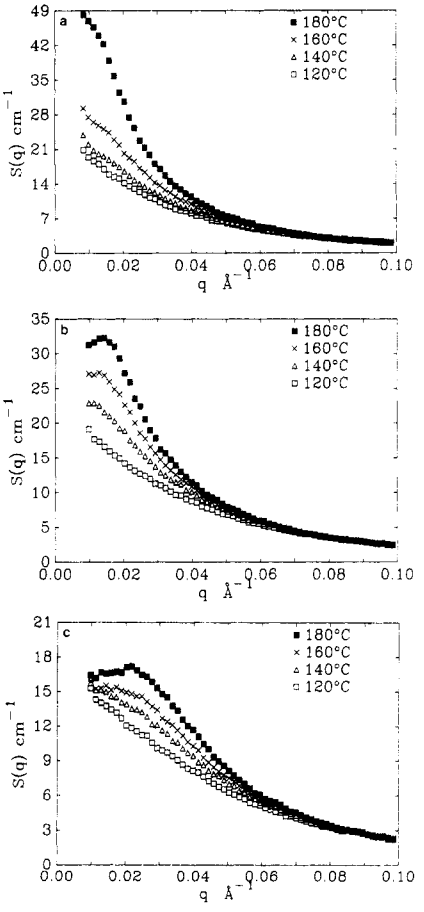

Figure 5. (a) $S(q)$ versus q at different temperatures for sample 25MR. (b) $S(q)$ versus q at different temperatures for sample 50MR. (c) $S(q)$ versus q at different temperatures for sample 125MR.

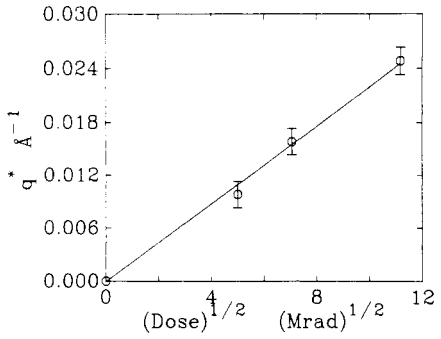

Figure 6. Plot of the position of the maximum in $S(q)$, q^*, versus $(\text{dose})^{1/2}$.

Table IV

sample	q^* (Å^{-1})	T_s (°C)	sample	q^* (Å^{-1})	T_s (°C)
0MR	0	149	50MR	0.0158	255
25MR	0.0098	240	125MR	0.0248	430

Parts a–c of Figure 5 are plots of $S(q)$ versus q for samples 25MR, 50MR, and 125MR, respectively, for a number of different temperatures. The behavior for the irradiated samples is qualitatively different than for the unirradiated sample. The first point to notice is that at the equivalent temperatures the scattered intensity is greatly reduced for the irradiated samples versus the unirradiated sample. In addition, the scattering instead of increasing in intensity at $q = 0$ is diverging at a nonzero q vector (this is especially visible in sample 125MR at the highest temperatures). The position of the peak (i.e. the value of q^*) can be determined from parts b and c of Figure 5 at the highest temperatures. Unfortunately the value of q^* for sample 25MR was close to the small q limit for the configuration of the SANS instrument used in these experiments so the peak for sample 25MR is not well defined. The values of q^* are given in Table IV.

The number of cross-links in the sample is proportional to the dose, and hence the number of units between cross-links should be inversely proportional to the dose

$$N_c^{-1} \sim D \tag{17}$$

This combined with eq 9 indicates that a plot of q^* versus the square root of the dose, $D^{1/2}$, should be linear. Figure 6 is such a plot. The linear relationship between q^* and $D^{1/2}$ appears to be valid for the samples studied in this paper. The error bars in Figure 6 are estimated by assuming that the peak position could be in error by one data point in the scattering curve on either side of the values given in Table IV (i.e. $q^* = \pm 0.0015$ Å^{-1}). The peak for the 0MR sample is assumed to be at $q = 0$. The line drawn through the data in Figure 6 is a linear least-squares fit to the data with the intercept set equal to zero. The slope of the line q^* versus $N_c^{-1/2}b^{-1}$ should be 5.42 according to eq 9. Using the average values for N_c calculated in Table II and the average value of $b \approx 7$ Å for PSD/PVME,[1,2] the least-squares slope of the line q^* versus $N_c^{-1/2}b^{-1}$ is 2.30. This is significantly smaller than the value of 5.42 predicted by de Gennes, indicating that the "internal ridigity" constant, C, in eq 8 is not accurate for this system. In other words, the measured peak in the scattering function occurs at a q vector about a factor of 2 smaller than the value predicted by de Gennes in eq 9. Even when accounting for the large uncertainty in N_c, the value of C is still significantly different from the value calculated by de Gennes. For example, if N_c is allowed to vary by a factor of 2 in either direction then calculated value of C varies between 1.63 and 3.25. Still, this discrepancy is probably not very

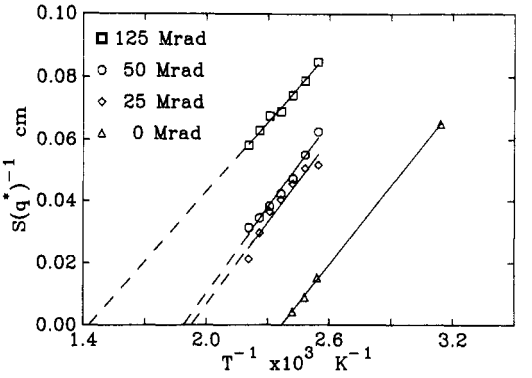

Figure 7. Plot of $S(q^*)^{-1}$ versus T^{-1} for the samples 0MR, 25MR, 50MR, and 125MR.

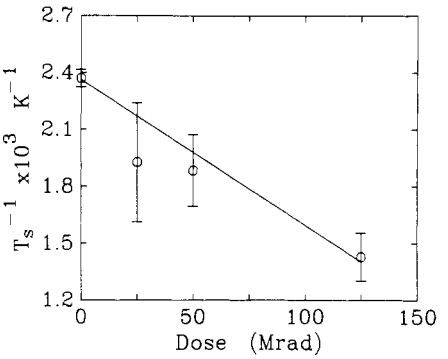

Figure 8. Plot of the inverse spinodal temperature, T^{-1}, versus dose.

significant since de Gennes is careful to point out the calculation of C is very approximate. In addition, part of the difference may be due to the presence of A–A and B–B cross-links in the blends which are not accounted for in the theory. The fact that the composition of the blend is not $\phi = 0.5$ as used in theory would probably be only a minor adjustment. If we assume that the q^2 and q^{-2} terms in eq 8 have the same dependence on ϕ as they do for a block copolymer, then the shift in q^* for a change in composition from 0.5 to 0.3 is only about 5%. The most important point to emphasize is that the relation given by eq 9 predicts the correct dependence of q^* on N_c even if the proportionality constant is not completely accurate.

Figure 7 is a plot of $S(q^*)^{-1}$ ($S(0)^{-1}$ for sample 0MR) versus T^{-1} which should allow extrapolation to the spinodal temperature, T_s. The lines in Figure 7 are linear least-squares fit to the data, and with the assumption of mean field behavior as given in eq 12, the spinodal temperature is the temperature where $S(q^*)^{-1} = 0$. The extrapolated spinodal temperatures are given in Table IV. The spinodal temperatures increase rapidly with increasing dose, greatly enlarging the temperature range of the single region of the phase diagram. The spinodal temperature increases from 149 °C for the unirradiated blend to an extrapolated value of 430 °C for sample 125MR. The mean field exponent of $\nu = 1$ for $S(q^*)$ was assumed to be valid and within the accuracy of the experiment the data in Figure 7 obey eq 12. The relation between the spinodal temperature and N_c is given by eq 13, and if we again use the relation $N_c^{-1} \sim D$, then a plot of T_s^{-1} versus dose should be a straight line. Figure 8 is a plot of T_s^{-1} versus dose. The error bars in Figure 8 correspond to one standard deviation in the value of T_s^{-1} determined from the least-squares fit in Figure 7. The line in Figure 8 is a linear least-squares fit to the data with each of the values of T_s^{-1} weighted by its respective inverse standard deviation squared. The data appear to follow the linear relationship given by eq 13

although the error in sample 25MR is quite large because of the scatter of the data in Figure 7 for this sample. It is possible that at a dose of 25 Mrad the presence of dangling ends is affecting the data and hence the extrapolated value of T_s.

It is worthwhile examining the scattering curves for the irradiated samples presented in parts a–c of Figure 5 in a little more detail. When the curves are compared to the theoretical ones in Figure 1, the most striking difference, other than the shift in q^* discussed above, is that the theory predicts that $S(0) = 0$ which is not observed experimentally. de Gennes made the assumption in the derivation of the scattering function that the sample was cross-linked under conditions of "good miscibility" which may be difficult to achieve experimentally. The cross-linking in the work presented in this paper was done in the single phase, but there were still concentration fluctuations present during cross-linking resulting in a cross-linked sample which has a finite amount of scattering at $q = 0$, comparable to the scattering from a linear blend at the temperature of cross-linking. Another source of zero angle scattering would be small amounts of incompletely cross-linked material since no attempt was made to remove any such extractables prior to the SANS experiments. It should be noted that excess zero angle scattering has also been observed for diblock copolymers in the single phase region.[7]

In a somewhat ad hoc attempt to account for the effect of the concentration fluctuations present at the temperature of cross-linking the scattering curve for the uncross-linked specimen (sample 0MR) at 45 °C (the approximate temperature at cross-linking) was subtracted from the irradiated samples. The results of this subtraction are presented in parts a–c of Figure 9. Clearly the data in Figure 9 now resemble the theoretical scattering curves in Figure 1 more closely, at least in a qualitative sense. The validity of this subtraction is difficult to argue rigorously, and if one plots the inverse of the subtracted scattered intensity at q^* versus T^{-1}, the data do not behave in a consistent manner as it did for the unsubtracted data. This indicates that the effect of the concentration fluctuations at the temperature of cross-linking cannot be simply subtracted from the data. Nevertheless, the subtraction does point out very clearly where the theory appears to fall short in explaining actual experimental results. In addition the presence of a peak in the scattering data for sample 25MR is clearly seen in Figure 9a while it was not clearly defined in Figure 5a.

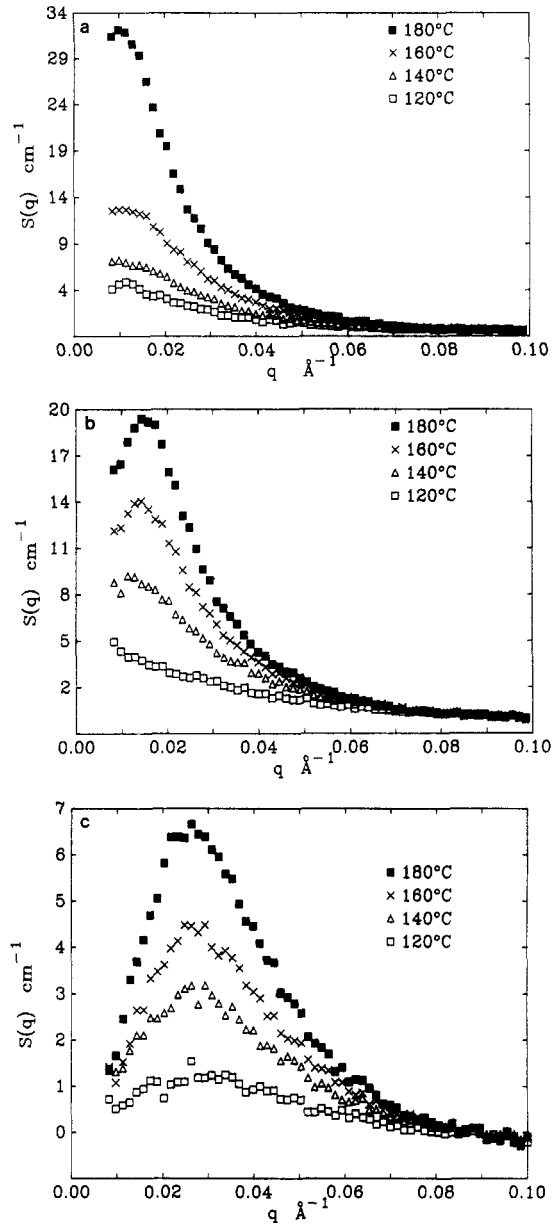

Figure 9. (a) Plot of the scattering function with the scattering from the linear blend at the temperature of cross-linking (45 °C) subtracted versus q at the different temperatures for sample 25MR. (b) Plot of the scattering function with the scattering from the linear blend at the temperature of cross-linking (45 °C) subtracted versus q at the different temperatures for sample 50MR. (c) Plot of the scattering function with the scattering from the linear blend at the temperature of cross-linking (45 °C) subtracted versus q at the different temperatures for sample 125MR.

Conclusions

The effect of radiation cross-linking on the phase diagram and scattering function for a compatible linear blend of PSD and PVME has been examined by SANS. An attempt has also been made to correlate the findings with a theory for such systems that has been presented by de Gennes.

The SANS curves for the crosslinked blends exhibits peak at a nonzero q vector, q^*, which increases in intensity with increasing temperature. The value of q^* varies linearly with the square root of the radiation dose and hence inversely with $N_c^{1/2}$ as predicted by de Gennes. The absolute value of q^* measured seems to be smaller than predicted by a factor of about 2, indicating that the value of the "internal rigidity" estimated by de Gennes is too large. A plot of the inverse scattered intensity at q^*, $S(q^*)^{-1}$ versus T^{-1}, gives a linear relationship which allows extrapolation to the spinodal temperature. The inverse of the measured spinodal temperature varies linearly with the radiation dose and inversely with N_c also as predicted by de Gennes. This results in a large increase in the single phase region of the phase diagram with increasing radiation dose. The spinodal temperature increases from 140 °C for the unirradiated blend to an extrapolated value of 430 °C for the sample with a dose of 125 Mrad. The effect of cross-linking on the phase diagram for polymer blends is summarized in Figure 10. It should be noted that the increase in the single phase region of the phase diagram is due to the presence of A–B cross-links and is not a result that will necessarily apply to cases where only A–A or B–B cross-links are present.

The theory by de Gennes does not account for the effect of finite concentration fluctuations present in the blend during cross-linking and predicts that $S(q = 0) = 0$ which

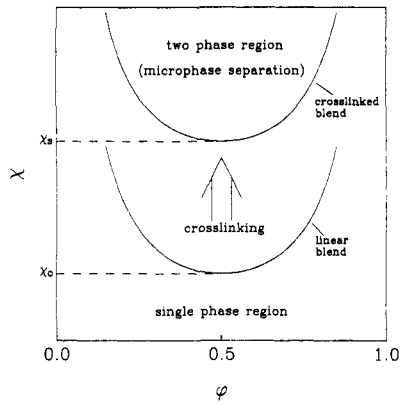

Figure 10. Schematic phase diagram showing the effect of cross-linking. Note the single phase region of the phase diagram is increased by cross-linking.

is not observed experimentally.

Acknowledgment. We wish to thank Drs. C. Glinka and J. Gotaas at the National Bureau of Standards for help with the SANS instrument and J. Humphries for preforming the irradiation of the samples. In addition we wish to thank Dr. Charles C. Han for many enlightening discussions and use of the temperature stage for the SANS instrument.

Registry No. PVME, 9003-09-2; neutron, 12586-31-1.

References and Notes

(1) Han, C. C.; Okada, M.; Muroga, Y.; McCrackin, F. L.; Bauer, B. J.; Tran-Cong, Q. *Polym. Eng. Sci.* **1986**, *26*, 2.
(2) Shibayama, M.; Yang, H.; Stein, R. S.; Han, C. C. *Macromolecules* **1985**, *18*, 2179.
(3) Jelenic, J.; Kirste, R. G.; Oberthur, R. C.; Schmitt-Streker, S.; Schmitt, B. J. *Makromol. Chem.* **1984**, *185*, 129.
(4) Bates, F. S.; Dierker, S. B.; Wignall, G. D. *Macromolecules* **1986**, *19*, 1938.
(5) Benoit, H.; Wu, W.; Benmouna, M.; Mozer, B.; Bauer, B.; Lapp, A. *Macromolecules* **1986**, *18*, 986.
(6) Bates, F. S. *Macromolecules* **1985**, *18*, 525.
(7) Bates, F. S.; Hartney, M. A. *Macromolecules* **1985**, *18*, 2478.
(8) de Gennes, P.-G. *Scaling Concepts in Polymer Physics*; Cornell University: Ithaca, NY, 1979.
(9) Benoit, H.; Benmouna, M. *Macromolecules* **1984**, *17*, 535.
(10) Leibler, L. *Macromolecules* **1980**, *13*, 1602.
(11) Ohta, T.; Kawasaki, K. *Macromolecules* **1986**, *19*, 262.
(12) Olvera de la Cruz, M.; Sanchez, I. C. *Macromolecules* **1986**, *19*, 2501.
(13) De Gennes, P. G. *J. Phys. (Les Ulis, Fr.)* **1979**, *40*, L-69.
(14) Han, C. C.; Bauer, B. J.; Clark, J. C.; Muroga, Y.; Matushita, Y.; Okada, M.; Tran-Cong, Q., submitted for publication in *Polymer*.
(15) Yang, H. S.; Hadziioannou, G.; Stein, R. S. *J. Polym. Sci., Polym. Phys. Ed.* **1983**, *21*, 159.
(16) Coleman, M. M.; Serman, C. J.; Painter, P. C. *Macromolecules* **1987**, *20*, 226.
(17) Frisch, H. L.; Klempner, D.; Yoon, H. K.; Frisch, K. C. *Macromolecules* **1980**, *13*, 1016.
(18) Sperling, L. H. *Interpenetrating Polymer Networks and Related Materials*; Plenum: New York, 1981.
(19) Bauer, B. J.; Briber, R. M.; Han, C. C. *Polym. Prepr. (Am. Chem. Soc., Dir. Polym. Chem.)* **1987**, *28*(2), 169.
(20) Bauer, B. J; Briber, R. M.; Han, C. C., submitted for publication in *Macromolecules*.
(21) Dole, M. *The Radiation Chemistry of Macromolecules*; Academic: New York, **1972**; Vol. I, II.
(22) Kells, D. I. C.; Guillet, J. E. *J. Polym. Sci., Polym. Phys. Ed.* **1969**, *7*, 1895.
(23) Schulz, G. V. *Z. Phys. Chem., Abt. B* **1939**, *B43*, 25.
(24) Zimm, B. H. *J. Chem. Phys.* **1948**, *16*, 1099.
(25) Flory, P. J. *J. Chem. Phys.* **1941**, *9*, 660; **1942**, *10*, 51.
(26) Huggins, M. L. *J. Chem. Phys.* **1941**, *9*, 440.
(27) Benoit, H., private communication.
(28) Stanley, H. E. *Introduction to Phase Transitions and Critical Phenomena*; Oxford University: New York, 1971.
(29) Bauer, B. J.; Hanley, B.; Muroga, Y., submitted for publication in *Polym. Commun.*
(30) Certain equipment, instrument, or materials are identified in this paper in order to adequately specify the experimental details. Such identification does not imply recommendation by the National Bureau of Standards nor does it imply the materials are necessarily the best available for the purpose.
(31) Duffy, D. *Ind. Eng. Chem.* **1958**, *50*, 1267.